



HAL
open science

Effects of temperature and p CO₂ on the respiration, biomineralization and photophysiology of the giant clam *Tridacna maxima*

Chloé Brahmi, Leila Chapron, Gilles Le Moullac, Claude Soyez, Benoît Beliaeff, Claire E Lazareth, Nabila Gaertner-Mazouni, Jeremie Vidal-Dupiol

► To cite this version:

Chloé Brahmi, Leila Chapron, Gilles Le Moullac, Claude Soyez, Benoît Beliaeff, et al.. Effects of temperature and p CO₂ on the respiration, biomineralization and photophysiology of the giant clam *Tridacna maxima*. 2021. hal-03239758

HAL Id: hal-03239758

<https://hal.science/hal-03239758>

Preprint submitted on 27 May 2021

HAL is a multi-disciplinary open access archive for the deposit and dissemination of scientific research documents, whether they are published or not. The documents may come from teaching and research institutions in France or abroad, or from public or private research centers.

L'archive ouverte pluridisciplinaire **HAL**, est destinée au dépôt et à la diffusion de documents scientifiques de niveau recherche, publiés ou non, émanant des établissements d'enseignement et de recherche français ou étrangers, des laboratoires publics ou privés.

1 Effects of temperature and $p\text{CO}_2$ on the respiration, biomineralization
2 and photophysiology of the giant clam *Tridacna maxima*

3
4

5 Running title: Climate change effects on *T. maxima*

6

7 Chloé Brahmi^{1*}, Leila Chapron^{2,3}, Gilles Le Moullac², Claude Soyez², Benoît Beliaeff², Claire E.
8 Lazareth⁴, Nabila Gaertner-Mazouni¹, Jeremie Vidal-Dupiol^{2,5}

9

10

11 ¹ Université de la Polynésie française, Ifremer, ILM, IRD, EIO UMR 241, Faa'a, Tahiti, French Polynesia

12 ² Ifremer, UMR 241 EIO, Labex Corail, Centre du Pacifique, BP 49, 98719 Taravao, Tahiti, French
13 Polynesia

14 ³ Sorbonne Université, CNRS, Laboratoire d'Ecogéochimie des Environnements Benthiques, LECOB,
15 F-66650, Banyuls-sur-mer, France

16 ⁴ Biologie des Organismes et Écosystèmes Aquatiques (BOREA), Muséum National d'Histoire
17 Naturelle, Sorbonne Université, Université de Caen Normandie, Université des Antilles, CNRS, IRD, 61
18 rue Buffon, CP 53, 75231 Paris, France

19 ⁵ IHPE, Univ. Montpellier, CNRS, Ifremer, Univ. Perpignan Via Domitia, Montpellier France

20

21 * Corresponding author: chloe.brahmi@upf.pf

22 **Abstract**

23 Such as many other reef organisms, giant clams are today confronted to global change effects and can
24 suffer mass bleaching or mortality events mainly related to abnormally high seawater temperatures.
25 Despite its strong ecological and socio-economical importance, its responses to the two most alarming
26 threats linked to global change (i.e., ocean warming and acidification) still need to be explored. We
27 investigated physiological responses of 4-years-old *Tridacna maxima* specimens to realistic levels of
28 temperature and partial pressure of carbon dioxide ($p\text{CO}_2$) (+1.5°C and +800 μatm of CO_2) predicted
29 for 2100 in French Polynesian lagoons during the warmer season. During a 65-days crossed-factor
30 experiment, individuals were exposed to two temperatures (29.2°C; 30.7°C) and two $p\text{CO}_2$ (430 μatm ;
31 1212 μatm) conditions. Impact of each parameter and their potential synergetic effect were evaluated
32 on respiration, biomineralization and photophysiology. Kinetics of thermal and acidification stress were
33 evaluated by performing measurements at different times of exposure (29, 41, 53, 65 days). At 30.7°C,
34 the holobiont O_2 production, symbiont photosynthetic yield, and density were negatively impacted. High
35 $p\text{CO}_2$ had a significant negative effect on shell growth rate, symbiont photosynthetic yield and density.
36 Shell microstructural modifications were observed from 41 days in all temperature and $p\text{CO}_2$ conditions.
37 No significant synergetic effect was found. Today thermal conditions (29.2°C) appeared to be sufficiently
38 stressful to induce a host acclimatization process. All these observations indicate that temperature and
39 $p\text{CO}_2$ are both forcing variables affecting *T. maxima* physiology and jeopardize its survival under
40 environmental conditions predicted for the end of this century.

41

42 **Keywords:** Thermal stress, ocean acidification, respiration, photosynthetic yield, giant clam, symbionts

43 1. Introduction

44 Since the industrial revolution, human activities released gigatons of CO₂ in the atmosphere, which
45 participate to global change (Broecker et al., 1979; Caldeira and Wickett, 2003; Sabine et al., 2004; Zeebe
46 et al., 2008; IPCC, 2014). Due to the “greenhouse gas” property of CO₂, terrestrial and sea surface
47 temperature rise constantly (i.e., global warming). According to the last Intergovernmental Panel on
48 Climate Change report (IPCC, 2018), human-induced warming had already reached about +1°C above
49 pre-industrial levels and the panel predicts +1.5°C around 2040 if the current warming rate continues.
50 Enrichment of dissolved CO₂ in the ocean modifies the carbonate chemistry by depressing carbonate
51 ion concentration ([CO₃²⁻]) and releasing protons which respectively decrease calcium carbonate
52 saturation state (Ω) and seawater pH (Kleypas et al., 1999; Caldeira and Wickett, 2003) (i.e., ocean
53 acidification). Indeed, pH had already decreased by 0.1 pH unit since the pre-industrial revolution and
54 the decrease may reach -0.3 to -0.4 pH unit by 2100 (according to the median scenario RCP 4.5, IPCC,
55 2014).

56 Since CO₃²⁻ is a carbonate ion form involved in biologically controlled calcification process (i.e.,
57 biomineralization) (Orr et al., 2005), marine organisms which form calcium carbonate structures (e.g.,
58 exoskeleton, shell, test, spicule), such as scleractinian corals, mollusks, and echinoderms are
59 particularly vulnerable to ocean acidification (Hoegh-Guldberg et al., 2007; Ries et al., 2009; Kroeker et
60 al., 2013; Gazeau et al., 2013). Among marine calcifying mollusks, negative impacts of temperature and
61 pCO₂ have been demonstrated on the survival, growth, biomineralization processes, and others key
62 physiological functions on different stages of their life cycle (Bougrier et al., 1995; Kurihara, 2008;
63 Gazeau et al., 2010, 2011; Schwartzmann et al., 2011; Rodolfo-Metalpa et al., 2011; Talmage and
64 Gobler, 2011; Watson et al., 2012; Liu et al., 2012; Kuhihara et al., 2013; Fitzer et al., 2014; Le Moullac
65 et al., 2016a,b; Wessel et al., 2018). However, effects of each stressor and their potential synergetic
66 effect on giant clam physiology are still poorly known.

67 Giant clams live in obligatory symbiosis with photosynthetic dinoflagellates of the family
68 Symbiodiniaceae (Holt et al., 2014; LaJeunesse et al., 2018). Different giant clam species, i.e., *Tridacna*
69 *maxima*, *Tridacna crocea*, *Tridacna noae* and *Tridacna squamosa*, have been found to associate with
70 different Symbiodiniaceae genera, i.e., *Symbiodinium* (formerly clade A, LaJeunesse et al., 2018),
71 *Cladocopium* (formerly clade C, LaJeunesse et al., 2018) and *Durusdinium* (formerly clade D,
72 LaJeunesse et al., 2018) (Pinzón et al., 2011; DeBoer et al., 2012; Ikeda et al., 2017; Lim et al., 2019).
73 Hereafter, the symbiotic Symbiodiniaceae are named “symbionts”. In giant clams, symbionts are located
74 extracellularly inside a tubular system called “Z-tubules” found in the outer epithelium of the mantle and
75 connected to the stomach (Norton et al., 1992; Holt et al., 2014). These mixotrophic organisms acquire
76 nutrients from heterotrophic (via seawater filtration) and symbionts photo-autotrophic pathways (Klumpp
77 et al., 1992; Hawkins and Klumpp, 1995). Nutrients provided by symbionts (such as glucose, Ishikura et
78 al., 1999) may account for a major part of the clam energy needs depending on the species and life
79 stage (Trench et al., 1981; Klumpp et al., 1992; Klumpp and Lucas, 1994; Klumpp and Griffiths, 1994;
80 Hawkins and Klumpp, 1995; Elfving et al., 2002; Yau and Fan, 2012; Holt et al., 2014; Soo and Todd,
81 2014). Like symbiotic coral species, bleaching events affecting giant clam have been recorded several
82 times in the Indo-Pacific Ocean (Adessi, 2001; Buck et al., 2002; Leggat et al., 2003; Andréfouët et al.,

83 2013; Junchompoo et al., 2013) mainly due to seawater temperature increase by a few degrees above
84 the seasonal maximum (Adessi, 2001; Andréfouët et al., 2013). Bleaching process results from the
85 symbiosis breakdown via the loose of symbiotic Symbiodiniaceae (Buck et al., 2002; Leggat et al.,
86 2003).

87 In French Polynesia, *Tridacna maxima* species (Röding, 1798) is one of the most emblematic
88 and patrimonial organisms. They represent an important food resource for inhabitants of remote atolls
89 and giant clam fishery and sustainable aquaculture activities generate substantial incomes for local
90 fishermen and farmers (Van Wysberge et al., 2016; Andréfouët et al., 2017). However, wild and
91 cultivated giant clam stocks are largely threatened by environmental disturbances such as abnormally
92 high sea surface temperature inducing mass mortality events as reported in Tuamotu atolls by Adessi
93 (2001) and Andréfouët et al. (2013). More recently, two mass bleaching events occurring in Reao and
94 Tatakoto (Tuamotu islands) were linked to a prolonged high lagoonal temperature ($\geq 30^{\circ}\text{C}$ over several
95 weeks) of these semi-closed atolls (Andréfouët et al., 2017; Fig. S1). All these observations strongly
96 indicate that temperature is an important stressor for giant clams. Besides the ecological consequences,
97 giant clam mass bleaching and mortality cause a significant loss of incomes for the islanders.

98 Despite their ecological and socio-economic importance, effects of thermal stress and
99 acidification on giant clams still need to be investigated. Thermal stress has shown to decrease
100 fertilization success (Amstrong, 2017) in *Tridacna maxima* and oxygen production and respiration rates
101 in *T. gigas* and *T. deresa* species (Blidberg et al., 2000). In contrast, an increase of respiration with a
102 high photosynthetic rate in the holobiont was reported for *T. squamosa* (Elfving et al., 2001). Thermal
103 stress also reduces the abundance of symbionts in *T. gigas* (Leggat et al., 2003) even after only 12h of
104 exposure in *T. crocea* (Zhou et al., 2018) and a decrease of photosynthate export from symbionts to the
105 host (Leggat et al., 2003). In *T. maxima*, heat stress induced changes of fatty acid composition and lipid
106 pathways and ROS (Reactive Oxygen Species) scavenger overexpression (Dubousquet et al., 2016).
107 Combined to high light intensities, heat stress caused a decrease of the cell size of remaining symbionts
108 and of their chlorophyll content (Buck et al., 2002). Recent studies demonstrated that low pH seawater
109 with high nutrient concentration could have variable effects on growth on four species of *Tridacna* genus
110 (Toonen et al., 2012). Moreover, Watson (2015) showed that high light irradiance condition limits the
111 impact of $p\text{CO}_2$ on shell growth. Regarding the potential synergetic effect of temperature and $p\text{CO}_2$
112 parameters, the only study ever carried out showed that ocean warming and acidification may reduce
113 survival in *T. squamosa* juveniles (Waston et al., 2012). To our knowledge, no study had already
114 investigated impact of both parameters, and their potential synergetic effect, on several key
115 physiological parameters of both *Tridacna maxima* host and its symbionts. To fill this gap, our
116 experimental approach was designed to better understand the physiological mechanisms underlying the
117 response of giant clams to global climate changes.

118 Based on a 65 days crossed-factor experiment, we investigated physiological responses of 4-years-old
119 *Tridacna maxima* specimens to temperature and $p\text{CO}_2$ conditions in the French Polynesian lagoons
120 during the today warmer season and those predicted for 2100 by the IPCC 2014: $+1.5^{\circ}\text{C}$ (RCP 4.5
121 scenario) and $+800 \mu\text{atm}$ of CO_2 (RCP 8.5 scenario). Effect of each parameter and their potential
122 synergetic effect were evaluated on respiration, biomineralization, and photophysiology by analyzing

123 the holobiont O₂ production and respiration, growth rate and ultrastructure of the shell and symbiont
124 density and photosynthetic yield. In addition, the kinetics of thermal and acidification stress were
125 accessed by performing analyses at different time of exposure (i.e., 29, 41, 53, 65 days).

126

127 **2. Materials and Methods**

128 *2.1. Biological material*

129 *Tridacna maxima* specimens of 4-years-old, 5-6 cm height and brownish/dark-green color, were
130 collected in early January 2016 from the cultivated stock in Reao lagoon (Tuamotu islands) and exported
131 to the Centre Ifremer du Pacifique in Tahiti where they were acclimatized in outdoor tank with running
132 seawater. Each individual was placed onto a petri dish on which byssal gland further developed for
133 fixation. All individuals directly opened up right after their transfer into the outdoor tank. No visual sign
134 of stress was observed during the acclimation period except for 4 individuals which died within the first
135 3 days (corresponding to a 2% mortality rate). Specimens used in this study were collected and held
136 under a special permit (MEI #284) delivered by the French Polynesian government.

137

138 *2.2. Experimental design and rearing system*

139 To study the impact of temperature, pCO₂, and their putative synergetic effect on the physiology of the
140 giant clams and their symbionts, four experimental conditions were set up by applying two temperatures
141 (29.2°C and 30.7°C) and two levels of pCO₂ (430 ±22 μatm and 1212 ±35 μatm). The tested conditions
142 were: (1) control: 29.2°C 430 μatm, (2) acidification stress: 29.2°C 1212 μatm), (3) thermal stress:
143 30.7°C 430 μatm, (4) acidification and thermal stress: 30.7°C 1212 μatm (Table 1).

144 After a 3 weeks acclimation period in an outdoor tank, 96 clams were randomly distributed in
145 experimental tanks one week before starting the experiment. For each condition, we used a 500 L tank
146 containing 4 tanks of 30 L (ecological replicates) renewed at a flow rate of 50 L/h (seawater pumped in
147 the lagoon). Each 30 L tank contained 6 clams (biological replicates). To avoid physiological shock,
148 targeted temperature and pCO₂ values were linearly achieved over 7 days. The light was set to obtain
149 a Photosynthetically Active Radiation (PAR) of 200 ± 20 μmol of photons. m⁻².s⁻¹ on a 12 h:12 h light/dark
150 photoperiod. To evaluate the kinetics of the thermal and/or acidification stress, analyses were performed
151 at 4 different times of exposure, i.e., 29, 41, 53 and 65 days. In total, 64 clams were used for data
152 acquisition corresponding to 4 individuals per condition (1 individual per 30 L tank) and per time of
153 exposure.

154

155 *2.3. Monitoring of temperature, pH and water quality*

156 To insure the stability of experimental conditions, temperature and pH parameters were measured twice
157 a day for each tank at 8:00 am and 4:00 pm using a mercury thermometer (certified ISO 9001, ±0.1°C
158 accuracy) and a pH-meter Consort P603 (±0.01 accuracy). Total alkalinity (TA) was weekly titrated using
159 a 0.01 N HCl solution and a titrator (Schott Titroline Easy). Levels of pCO₂ and aragonite saturation
160 state were calculated from temperature, pH (NBS scale), salinity and mean TA using the CO₂ Systat
161 software (van Heuven et al., 2009). All parameters including seawater carbonate chemistry are reported
162 in Table 1.

163

164 *2.4. Holobiont O₂ consumption and production measurements*

165 Giant clams were placed in an ecophysiological measurement system (EMS) to monitor O₂ consumption
166 and production. The EMS consisted in five open-flow chambers. Four giant clams were individually
167 placed into 4 chambers while an empty shell was placed into a fifth chamber used as a control. EMS
168 chambers contained water at the same temperature and pCO₂ conditions as in the experimental tanks.
169 The light energy and photoperiod conditions were the same as for the acclimation tanks. Flow rate in all
170 chambers was constantly maintained at 12 L.h⁻¹. Each chamber was equipped with a two-way
171 electromagnetic valve activated by an automaton (FieldPoint National Instruments). When the electro-
172 valve was opened, the water released from the chamber was analyzed for 3 min using an oxygen sensor
173 (OXI 538, Cellox 325, WTW, Weilheim, Germany) to quantify dissolved oxygen. Oxygen measurements
174 were performed over 48 h. The first 8 hours of measurement were discarded due to the animal
175 acclimatization to the chamber. In each chamber, the cycle was completed within 3 min: the first 2 min
176 served to stabilize the measurement and an average of oxygen data was performed on the last minute
177 of acquisition. This cycle was followed by another time frame of 3 min in the control chamber following
178 the sequence: specimen #1, control, specimen #2, control, specimen #3, control, specimen #4, control.
179 Respiration rate (RR) and production rate (PR) were calculated from data obtained during night- and
180 day-time, respectively, using differences in oxygen concentrations between the control and experimental
181 chambers. RR and PR = V(O₁ - O₂), with O₁ the oxygen concentration in the control chamber, O₂ the
182 oxygen concentration in the experimental chamber, and V the water flow rate. RR and PR data were
183 normalized to tissue dry weight. Once normalized, the terminology becomes O₂ consumption for RR
184 and O₂ production for PR, both expressed in mg O₂.h⁻¹.g⁻¹ dry weight.
185 After O₂ production and O₂ consumption analyses were completed, a piece of the mantle was dissected
186 for further symbiont fluorescence and density analyses (see section 2.5). The remaining soft tissues
187 were frozen and lyophilized for RR and PR data normalization.

188

189 *2.5. Fluorescence and density measurements of symbionts*

190 Potential effect of temperature and pCO₂ conditions on the photophysiology of the symbionts was
191 studied by comparing fluorescence yield of photosystem II between all experimental conditions. After
192 clams were sacrificed, a 1 cm x 2 cm mantle fragment was dissected. The tissue fragment was gently
193 swiped using tissue paper to remove a maximum of mucus and symbionts were collected by doing 5
194 smears using a sterilized razor blade. Collected symbionts were diluted into 5 mL of 0.2 µm filtered-
195 seawater and placed at the obscurity for 10 min to inactivate the photosystem II before light excitation.
196 Samples were homogenized and 3 ml of the homogenate were collected, placed into a quartz-glass
197 cuvette and analyzed with AquaPen fluorometer (APC-100, Photon System Instruments®, Czech
198 Republic) at a 450 nm wavelength. The fluorescence at the steady state (F₀) and the maximal
199 fluorescence in the light (F_m) were measured. The apparent quantum yield of photosynthesis (Y)
200 reflecting the efficiency of photosystem II in the light acclimated state (Hoogenboom et al., 2006) was
201 calculated according to equation (Eqn 1).

202

$$Y = \frac{(F_0 - F_m)}{F_m} \quad (1)$$

203 In addition, symbiont densities were evaluated from mantle fragments. For each individual, a circular (5
204 mm diameter) piece of mantle was collected using a punch. The piece was weighted, grounded in 0.2
205 μm filtered seawater and homogenized. Then, 20 μL of the tissue extract were immediately collected
206 and placed into Mallassez cells for symbiont counting under optical microscope. For each sample,
207 counting was performed on four replicates (3 columns per replicate). Data are expressed in number of
208 symbionts/mg of mantle tissue.

209

210 *2.6. Calcein labelling for evaluating daily shell extension rate*

211 To study the impact of temperature and $p\text{CO}_2$ on shell growth rate, the mineralization front of giant clams
212 was marked using calcein fluorochrome which is irreversibly precipitated at the CaCO_3 mineralization
213 site. Before the experiment starts, giant clams were immersed in a 100 mg/L calcein solution (Sigma
214 Aldrich) (calcein diluted in 1 μm filtered-seawater) for 8 h in the dark. During the labelling procedure, the
215 bath of calcein solution was aerated using bubblers and a water current was created via pumps. Calcein-
216 labelled specimens were then placed into the experimental tanks. At the end of the experiment, for each
217 individual, a 5 mm thick section was cut along the maximal shell growth axis through the right valve
218 using a Swap Top Inland[®] diamond saw. All sections obtained were polished and observed under
219 epifluorescence ($\lambda_{\text{excitation}} = 495 \text{ nm}$, $\lambda_{\text{emission}} = 515 \text{ nm}$) with a Leitz Dialux[®] 22 microscope. The distance
220 between the fluorescent calcein mark and the edge of the shell formed during the experiment was
221 measured following the maximal growth direction. Daily shell extension rate (expressed in $\mu\text{m}/\text{day}$) was
222 obtained by dividing the measured distance by the number of days of incubation in experimental
223 conditions.

224

225 *2.7. Shell scanning electron microscopy study*

226 To characterize temperature and $p\text{CO}_2$ effect on the shell ultrastructure, a scanning electron microscopy
227 (SEM) study was carried out. For each individual, a 10 mm thick shell section was cut facing the section
228 used for calcein observations. The section was then fractured along the width, 2 cm below the growing
229 part of the shell (marginal part), using a small chisel and a hammer. Then, the apical fragment was
230 longitudinally fractured and one piece was sonicated in tap water for 10 s, air-dried and an additional
231 drying was done overnight at 35°C. Sample was placed on a stub covered with carbon tape, gold-coated
232 and observed at 15 kV using a Hitachi TM3030 SEM at the Université de la Polynésie française. For
233 each condition, and for each time of exposure, 2 samples were selected based on their daily extension
234 rate, i.e., samples showing the lowest and the highest rate. To evaluate the impact of temperature and/or
235 $p\text{CO}_2$ on the shell ultrastructure, SEM observations were performed for each specimen in two different
236 zones of the crossed-lamellar outer layer (Pätzold et al., 1991). Zone 1 corresponds to the shell formed
237 *in situ* (i.e., in the shell region located before the calcein mark) while zone 2 corresponds to the shell
238 formed during the experiment. Observations were made at the ultrastructural level and focused on the
239 aspect and integrity of the lamellae of the crossed-lamellar outer layer.

240

241 2.8. Statistical analyses and data processing

242 Normality of data distribution and homogeneity of variance were tested with the Shapiro-Wilk test and
243 the Bartlett test, respectively. Production and consumption of O₂ data followed the conditions of
244 application of parametric tests, but photosynthetic yields and symbiont densities were transformed using
245 Box Cox transformation while shell extension rates were square root to meet these conditions.
246 Comparisons were done using a three-way ANOVA with interaction where factors were time of
247 exposure, temperature and pCO₂. Tukey post hoc comparisons were done at $\alpha=0.05$ for all analyses.
248 Correlations between physiological parameters were tested using Pearson method with a threshold of
249 $r=0.25$ ($\alpha=0.05$).

250 For all physiological parameters, i.e., O₂ respiration, O₂ consumption, symbiont photosynthetic yield and
251 density, means (\pm s.d.) were calculated based on the 4 biological replicates for each condition and each
252 time of exposure. For the daily shell extension rate, means (\pm s.d.) were calculated for each condition
253 and each time of exposure.

254

255 3. Results

256 3.1. Effect of temperature and pCO₂ on the holobiont oxygen balance

257 For all sampling time (i.e., 29, 41, 53, 65 days), a cyclic pattern of O₂ production and consumption is
258 observed following the circadian cycle (Fig. 1). This pattern corresponds to oxygen photosynthetically
259 produced and heterotrophically consumed by the holobiont during the day and the night, respectively.
260 Mean values of normalized O₂ production and consumption are shown in Fig. 2. These values were
261 analyzed using a three-way ANOVA with 3 fixed factors: temperature, pCO₂, and the time of exposure
262 (Table 2). Tukey post hoc test results are reported in Table 3. The ANOVA indicates that oxygen
263 production of the holobiont during day-time is significantly altered at 30.7°C ($P=0.009$) but not at 1212
264 μ atm of CO₂ ($P=0.361$) (Table 2). In addition, O₂ production is higher at 29.2°C than at 30.7°C for all
265 times of exposure (Fig. 2A) and decreases along the experiment ($P=0.030$) (Table 2). The night-time O₂
266 consumption, however, is not significantly influenced by temperature ($P=0.590$) neither by pCO₂
267 ($P=0.361$) nor by time of exposure ($P=0.533$) and remains stable along the whole experiment (Fig.
268 2A,B). No interaction effect between the 3 tested factors is found to affect the holobiont oxygen balance
269 (Table 2).

270

271 3.2. Symbiont density and photosynthesis under different T°/pCO₂ conditions

272 After two months of exposure, the symbiont photosynthetic yield and density are significantly impacted
273 at 30.7°C ($P<0.0001$), high pCO₂ (1212 μ atm) ($P<0.0001$ and $P=0.05$, respectively), and by the time of
274 exposure ($P=0.021$ and $P=0.001$, respectively). During the whole experiment and for both pCO₂
275 conditions, the means of photosynthetic yield (Fig. 2C) and symbiont density (Fig. 2D) tend to be higher
276 at 29.2°C than at 30.7°C. However, an inter-individual variability is observed.

277 Concerning the interaction parameters, only interaction between temperature and time of exposure
278 parameters has a significant effect on the symbiont photosynthetic yield ($P=0.025$) (Table 2). No
279 parameter interaction is found to affect the symbiont density (Table 2).

280

281 *3.3. Negative effect of pCO₂ on daily shell extension rate*

282 Calcein mark was detectable in 55 over 64 shell sections. Statistical analyses on shell extension rate
283 data indicate that pCO₂ and the time of exposure have a significant effect on the shell extension rate
284 ($P=0.010$ and $P=0.007$, respectively) (Table 2). In the Fig. 2E, the mean values of shell extension rates
285 tend to be lower at high pCO₂.

286

287 *3.4. Relationship between physiological parameters*

288 To establish if relationships exist between the various physiological parameters measured, a correlation
289 matrix was generated (Table 4). The photosynthetic yield of symbionts is strongly correlated to their
290 density ($r=0.667$). O₂ production is also strongly correlated to symbiont density ($r=0.482$) and
291 photosynthetic yield ($r=0.331$). Concerning the circadian functioning of the holobiont, its nocturnal
292 oxygen need is strongly correlated to the diurnal O₂ production ($r=0.629$). No significant correlation is
293 found between shell extension rate and other physiological parameters.

294

295 *3.5. Effect of long-term exposure to temperature and pCO₂ on the shell microstructure*

296 Ultrastructural observations of shell fractures were done in two zones: zone 1 corresponding to the shell
297 formed *in situ* (i.e., before the experiment) and zone 2 corresponding to the shell formed in the
298 experimental conditions. The lamellae formed before the experiment (zone 1) are well-cohesive and
299 display an elongated shape, a smooth surface, and sharp or slightly rounded outlines (Fig. 3A,B,C). For
300 all experimental conditions, no difference between zone 1 and 2 is observed for all samples exposed for
301 29 days (Fig. 3A,D). From 41 days, the lamellae observed in the majority of shells formed during the
302 experiment (zone 2), in all temperature/pCO₂ conditions, appeared less cohesive with a pronounced
303 granular aspect of the surface (Fig. 3E,H) and/or less cohesive lamellae with a crazed-like aspect (Fig.
304 3F,I). Two states classifying ultrastructural differences between the shell formed before and during the
305 experiment were defined as follow: *i*) ND; no difference observed between zone 1 and 2, *ii*) D; difference
306 observed between zone 1 and 2. In total, 19 samples over 24 displayed differences in lamellae aspect
307 between both zones. Data are reported in Table 5.

308

309 *3.6. Effect of time of exposure on oxygen balance, biomineralization and symbionts photophysiology*

310 Time of exposure to thermal and acidification stress was shown to have a significant impact on O₂
311 production ($P=0.030$), photosynthetic yield ($P=0.021$), symbiont density ($P=0.001$) and shell growth rate
312 ($P=0.007$) (Table 2). Post hoc tests showed that the kinetics of thermal or acidification stress varies
313 depending on the physiological parameter measured: O₂ production and photosynthetic yield are
314 significantly different between 29 and 65 days while symbiont density and shell growth rate are both
315 impacted from 53 days of exposure (Table 3).

316

317 4. Discussion

318 In this present study, we investigated the physiological responses of *Tridacna maxima* (i.e., 4-years-old
319 specimens) to temperature and $p\text{CO}_2$ conditions in the French Polynesian lagoons under nowadays
320 warmer season conditions and those predicted for 2100 by the IPCC 2014 (+1.5°C and +800 μatm of
321 CO_2). Today thermal conditions are already and sufficiently stressful to induce an acclimatization
322 process pictured by a slight regulation of the symbiont density without the collapse of the photosynthesis.
323 However, if in the today conditions the giant clams are able to mount this acclimatory and efficient
324 response that enable to maintain their key physiological characteristics, the thermal and $p\text{CO}_2$ conditions
325 of tomorrow appear to be much more stressful and sufficient to induce strong disturbances of the two
326 key functional compartments of the giant clam, its phototrophic symbiosis and its biomineralization.
327 Indeed, the 30.7°C treatments have significantly impacted the holobiont by inducing a strong bleaching
328 response illustrated by the reduction of its O_2 production, symbiont density and photosynthetic yield.
329 High $p\text{CO}_2$ (+800 μatm of CO_2) was shown to alter the symbiont photosynthetic yield and density and to
330 affect its biomineralization process by decreasing the shell growth rate.

331

332 4.1. No synergetic effect between temperature and $p\text{CO}_2$ on giant clam and symbiont physiological 333 parameters

334 Increase of atmospheric CO_2 impacts both the seawater temperature and pH inducing ocean warming
335 and acidification (Sabine et al., 2004, IPCC, 2014). Therefore, the analysis of the synergetic effect of
336 both stressors on marine bivalve physiology is crucial. Watson et al. (2012) investigated the synergetic
337 effect of ocean acidification and warming on the survival of *T. squamosa* juveniles over a 60 days
338 crossed-factor experiment. They reported that the combination of the highest $p\text{CO}_2$ (+600 μatm of CO_2)
339 and both moderate and highest seawater temperatures (30.0°C and 31.5°C) resulted in the lowest
340 survival rate of giant clams (<20%). They concluded that increased ocean $p\text{CO}_2$ and temperature are
341 likely to reduce the survival of *T. squamosa* juveniles. In our study, no synergetic effect was detected
342 for all measured physiological parameters on *T. maxima*. Moreover, no mortality was observed in all
343 tested temperature/ $p\text{CO}_2$ conditions during the whole experiment which lead us to suggest that a
344 temperature of 30.7°C and a $p\text{CO}_2$ of 1212 μatm seem to be non-lethal, at least over 65 days of
345 exposure. However, we cannot exclude that some specimens, especially the totally bleached
346 individuals, may have died after a longer exposure to the experimental conditions.

347

348 4.2. Effect of temperature on holobiont oxygen balance, symbiont photophysiology and shell 349 ultrastructure

350 Temperature is a factor well-known to influence several physiological parameters in bivalves as it
351 regulates the metabolism of ectotherm organisms (Aldridge et al., 1995, Bougrier et al., 1995, Watson
352 et al., 2012, Gazeau et al., 2013; Le Moullac et al., 2016a; Latchère et al., 2017). However, since giant
353 clams live in symbiosis with photosynthetic symbionts (Klumpp et al., 1992; Klumpp and Griffiths, 1994;
354 Soo and Todd, 2014), the comparison at the metabolic level with non-symbiotic bivalves can be
355 audacious. Discussion on elevated temperature effect on the holobiont oxygen balance should therefore
356 integrate the effect on both giant clam and its symbionts (Jones and Hoegh-Guldberg, 2001). Even

357 though physiological and molecular response to thermal stress may differ, the comparison with
358 scleractinian corals, which are also symbiotic and calcifying organisms, makes sense to better
359 understand the impact of temperature on the holobiont physiology.

360 We observed that high temperature (+1.5°C) significantly reduces the holobiont O₂ production, the
361 density and the photosynthetic yield of symbionts from 29 days of exposure. Additionally, partial or total
362 bleaching was observed for the majority of individuals exposed to 30.7°C (at both ambient and high
363 pCO₂, Fig. S2). This suggests that thermal stress has a significant impact on the holobiont
364 photophysiology. The reduction of the symbiont photosynthetic yield could reflect a photoinhibition.
365 Photoinhibition was previously linked to the degradation of the D1 protein of the reaction center of the
366 photosystem II (PSII) altering the photosynthetic apparatus functioning in symbiotic corals and sea
367 anemone subjected to thermal stress (Warner et al., 1999; Smith et al., 2005; Richier et al., 2006;
368 Ferrier-Pagès et al., 2007). Diminution of photosynthetic activity reduces the symbiont O₂ production
369 and consequently, impacts the holobiont O₂ production. Comparable results were obtained from a 24-
370 hour experiment showing that an increase of 3°C affects the oxygen production of *Tridacna gigas* and
371 *Tridacna deresa* (Blidberg et al., 2000). Photoinhibition led to the production of reactive oxygen species
372 (ROS) by symbionts which are known to pass through cellular membranes, cause oxidative damages
373 (Lesser et al., 1990; Lesser, 1996; Downs et al., 2002) and impact the photosystem II (Richter et al.,
374 1990). Considering corals, a strong positive correlation between accumulation of oxidative damage and
375 coral bleaching was shown (Downs et al., 2002). Indeed, ROS such as hydrogen peroxide (H₂O₂) may
376 play a role of signaling molecule activating the symbiosis dissociation (Fitt et al., 2001; Smith et al.,
377 2005; Perez and Weis, 2006). Expulsion of symbionts by the host may be a strategy to limit oxidative
378 stress and damage to ultimately survive environmental stress (Downs et al., 2002; Perez and Weis,
379 2006). Two recent works support this hypothesis. One of Zhou et al. (2018) which related a decrease in
380 symbiont density in response to an excess of oxidative stress in thermally stressed *T. crocea*. A second
381 of Dubousquet et al. (2016) which showed that *T. maxima* overexpressed genes encoding ROS
382 scavengers in response to thermal stress. Interestingly, the cellular and molecular mechanisms
383 enhanced upstream the bleaching response seem similar between giant clams and corals and conduct
384 to the same phenomenon of symbiosis dissociation. However, since giant clams and corals display an
385 extra- and an intra-cellular symbiosis respectively, the mechanisms of the symbiosis dissociation must
386 differ. In every instance, this constitutes an interesting example of evolutionary convergence of a stress
387 response in two very distant organisms. In this context, it would be interesting to test if the bleaching
388 response in giant clam can be adaptive as it was proposed for corals (Fautin and Buddemeier, 2004)
389 and if variations in giant clam thermo-tolerance are correlated to the composition of the symbiotic
390 population (Baker, 2003).

391 Concerning the effect of temperature on the ultrastructure of the crossed-lamellar structure, the lamellae
392 formed in all experimental conditions in the first 29 days are well-cohesive with elongated shape and a
393 granular aspect which is consistent with the description made by Agbaje et al. (2017) in *T. deresa*.
394 However, after 29 days, the lamellae observed in the majority of shells formed in both temperature
395 conditions (whatever the pCO₂ condition) appeared to be less-cohesive with pronounced granular
396 aspect. We suggest that these features are due to a lack of organic matrix between the lamellae (i.e.,

397 inter-lamellar organic matrix) and embedding the nano-grains forming the first-order lamellae in the
398 crossed-lamellae structure (as described by Agbaje et al., 2017). Indeed, the biomineralization of
399 calcium carbonate structures involved the transport of ions (calcium, bicarbonates and protons) to the
400 mineralization site and the synthesis of macromolecules referred to as “organic matrix” (Allemand et al.,
401 2004). The organic matrix, consisting of 0.9% weight of *T. deresa* shell, and is mainly composed of
402 assemblage of macromolecules such as polysaccharides, glycosylated, and unglycosylated proteins
403 and lipids (Agbaje et al., 2017). These macromolecules are commonly found in molluscan shell organic
404 matrix (Marin et al., 2012) present as inter-crystalline envelope and around individual crystal units
405 (Harper, 2000). The formation of these macromolecules is energetically costly for mollusks such as
406 marine gastropods (Palmer, 1992). According to the conclusion made by Milano et al. (2016) in the non-
407 symbiotic bivalve *Cerastoderma edule*, we suggest that in our tested experimental temperature, while
408 respiration function is significantly altered, less energy is available and allocated to the synthesis of
409 macromolecules involved in biomineralization which may explained the lack of organic matrix embedded
410 into the giant clam shell.

411

412 4.3. Effect of $p\text{CO}_2$ on giant clam biomineralization and symbiont photophysiology

413 Ocean acidification is related to an increase of dissolved CO_2 in the seawater resulting in a modification
414 of carbonate chemistry equilibrium and a decrease of seawater pH. This phenomenon is known to affect
415 biomineralization process of marine calcifiers since the production of biocarbonate structures depends
416 on both calcium carbonate saturation state and on the ability to express proteins involved in
417 biomineralization (Fitzer et al., 2014). The $p\text{CO}_2$ is a well-known parameter to influence mollusk
418 calcification process in terms of growth rate, expression of gene encoding proteins involved in
419 biomineralization, and to alter the integrity of biocarbonate structures (Welladsen et al., 2010; Melzner
420 et al., 2011; Fitzer et al., 2014; Le Moullac et al., 2016b), even if counter examples exist (Ries et al.,
421 2009; Kroeker et al., 2010).

422 Concerning giant clams, our results indicate that in high $p\text{CO}_2$ condition (+800 μatm), shell extension
423 rate decreases significantly. This observation is in accordance with those obtained for giant clams in
424 three different experiments using various CO_2 enrichment level and exposure duration. Waters (2008)
425 and Watson (2015) have exposed juveniles *T. squamosa* to +200 μatm of CO_2 for 13 weeks and to +250
426 and +550 μatm of CO_2 for 8 weeks, respectively. Toonen et al. (2012) demonstrated that young
427 specimens of *T. maxima* and *T. squamosa* have lower shell growth rates, compared to those reported
428 in the literature under natural $p\text{CO}_2/\text{pH}$ conditions, when kept 1 year in +350 to +1000 μatm $p\text{CO}_2$
429 conditions.

430 As mentioned above, high $p\text{CO}_2$ condition (+800 μatm) affects giant clam shell growth rate but also
431 symbiont photosynthetic yield and density. Negative effect of $p\text{CO}_2$ on the shell growth rate may be
432 linked to (1) the aragonite saturation state which is lower at 1212 μatm than at 430 μatm and/or (2) an
433 alteration of symbiont photophysiology leading to a potential reduction of the ‘light-enhanced
434 calcification’ (LEC). Concerning the former, decline of coral calcification rate has been related to

435 modifications of carbonate chemistry due to a limitation of CO_3^{2-} ions available for calcification. Even if
436 corals may upregulate the pH at their mineralization site (Venn et al., 2013; Holcomb et al., 2014), the
437 decrease of coral calcification was also linked to a decline in pH in the calcifying fluid due to a lower
438 seawater pH (Ries et al., 2011; McCulloch et al., 2012). In our case, we suggest that giant clam *T.*
439 *maxima* exposed to high $p\text{CO}_2$ may allocate more energy to maintain a proper pH of the fluid in the
440 extra-pallial space for nucleation and deposition of aragonite since the $\Omega_{\text{aragonite}}$ at high $p\text{CO}_2$ is twice
441 lower than at ambient $p\text{CO}_2$ ($\Omega_{\text{aragonite}, 1212 \mu\text{atm}} = 2$, $\Omega_{\text{aragonite}, 430 \mu\text{atm}} = 4$). Regarding the light-enhanced
442 calcification (LEC) (Vandermeulen et al., 1972), this phenomenon observed in Symbiodiniaceae-host
443 symbiosis has been extensively described in corals and represents the capacity of symbionts to
444 stimulate the host calcification (Allemand et al., 2004). The symbionts stimulate the host metabolism
445 and calcification by providing energy resources and/or O_2 (Chalker and Taylor, 1975). Moreover,
446 symbionts may promote the aragonite precipitation by providing inorganic carbon, nitrogen and
447 phosphorus and by synthesizing molecules used as precursor for the synthesis of skeletal organic matrix
448 (Pearse and Muscatine, 1971; Cuif et al., 1999; Furla et al., 2000; Muscatine et al., 2005). They also
449 facilitate CaCO_3 precipitation by influencing the Dissolved Inorganic Carbon (DIC) equilibrium by
450 removing the CO_2 via photosynthesis (Goreau, 1959). Such phenomenon has been also described in
451 giant clams (Ip et al., 2006; Ip et al., 2017). In *T. squamosa*, LEC increases the pH and reduces the
452 ammonia concentration at the interface between the inner mantle and the shell in the extra-pallial fluid,
453 where the biomineralization occurs (Ip et al., 2006). Recently, Chew et al. (2019) reported a light-
454 enhanced expression of a carbonic anhydrase (i.e., CA4-like) in the inner mantle of *T. squamosa* and
455 suggested that this enzyme is involved in giant clam biomineralization by catalyzing the conversion of
456 HCO_3^- to CO_2 . In this context, an altered photophysiology of the symbiont can rationally alter LEC and
457 consequently results in a decrease of the shell growth rate. Finally, one can suggest that under
458 acidification stress, giant clam may reduce or stop some physiological functions such as
459 biomineralization and allocate more energy to essential functions to its survival. In our study,
460 temperature also altered photophysiology and holobiont O_2 production, but did not significantly affect
461 shell growth rate. Therefore, the most plausible hypothesis explaining the negative effect of $p\text{CO}_2$ on
462 shell growth rate may be related to the low aragonite saturation state at high $p\text{CO}_2$.

463 Concerning the effect of $p\text{CO}_2$ on the shell microstructural integrity, in the temperate bivalve *Mytilus*
464 *edulis*, an exposition to +150, +350 and +600 μatm of CO_2 for 6 months induced a disorientation in the
465 shell of the newly formed calcite crystals of the prismatic layer (Fitzer et al., 2014). In the giant clam *T.*
466 *maxima*, high $p\text{CO}_2$ had no negative effect on the integrity of the aragonitic lamellae of the crossed-
467 lamellar layer during the first 29 days of exposure. From 41 days of exposure, its potential impact
468 remains unresolved as differences were noticed in the shells formed under future high temperature, high
469 $p\text{CO}_2$ and even under today high temperature/ $p\text{CO}_2$ conditions. The fact that differences are reported
470 for shells formed in all experimental conditions from 41 days suggests that they may be due to a long-
471 term exposure to 29.2°C and 30.7°C.

472

473 This study enables the evaluation of *Tridacna maxima* physiological responses to temperature
474 and $p\text{CO}_2$ thresholds predicted at the end of this century. We demonstrated that high temperature has
475 a significant negative impact on symbiont densities and photosynthetic capacities, which induce a
476 decrease in holobiont O_2 production rate. We suggest that the observed decrease of holobiont O_2
477 production rate results from a decrease of symbiont O_2 production. Therefore, by influencing symbiont
478 physiology, the temperature may affect the energetic needs of the giant clam host. The high $p\text{CO}_2$ has
479 a negative impact on shell growth rate, symbiont densities and photosynthetic capacities. Shell
480 microstructure is affected neither by temperature nor by the $p\text{CO}_2$ in the first 29 days of exposure.
481 However, for all temperature/ $p\text{CO}_2$ conditions, a longer exposition (≥ 41 days) modified the shell
482 ultrastructure. These observations support our hypothesis that 29.2°C is a temperature that already
483 affects giant clam metabolism, at least over a long-term exposition. However, no synergetic effect was
484 found between temperature and $p\text{CO}_2$ parameters. All these observations suggest that temperature and
485 $p\text{CO}_2$ influence different physiological functions and that giant clam populations may dramatically suffer
486 from the temperature and $p\text{CO}_2$ conditions predicted for the next decades. To complement these results
487 on the effects of temperature on the holobiont, it is now essential to conduct further and integrative
488 analyses. This may include the definition of thermal optimum of *T. maxima* and the study of the
489 transcriptomic response of the giant clam and its symbiotic Symbiodiniaceae to thermal stress for
490 instance. All these analyses will allow a better understanding of the fundamental physiological processes
491 of the holobiont and its response to future changes. Attempted results may also help in adapting local
492 policies and management to maintain a sustainable exploitation of giant clam resource, especially in the
493 Eastern Tuamotu islands where bleaching events have been observed at an increasing and alarming
494 rate.

495

496 **Acknowledgments**

497 The authors would like to thank Celine Lafabrie for fruitful discussions and Mickael Mege and Alexia
498 Pihier for their technical assistance. Georges Remoissenet (Direction of Marine Resources of French
499 Polynesia) is thanked for sharing information about bleaching events in Eastern Tuamotu islands. The
500 Direction of Marine Resources and the Ministry of Economic Recovery, Blue Economy and Digital Policy
501 of French Polynesia are also thanked for according the special permit to collect and hold small
502 specimens of *Tridacna maxima* species. This study is set within the framework of the “Laboratoires
503 d’Excellence (LabEX)” TULIP (ANR-10-LABX-41).

504

505 **Competing interests**

506 The authors declare no competing interests.

507

508 **Funding**

509 This work was financially supported by the Ifremer institution (Politique de site program, GECO project)
510 and the University of French Polynesia (MAPIKO and CLAMS projects).

511

512 **References**

- 513 Adessi, L. (2001). Giant clam bleaching in the lagoon of Takapoto atoll (French Polynesia). *Coral Reefs*
514 **19**, 220.
- 515 Agbaje, O.B.A., Wirth, R., Morales, L.F.G., Shirai, K., Kosnik, M., Watanabe, T. and Jacob, D.E. (2017).
516 Architecture of crossed-lamellar bivalve shells: the southern giant clam (*Tridacna deresa*,
517 Röding, 1798). *R. Soc. Open Sci.* **4**, 170622
- 518 Allemand, D., Ferrier-Pagès, C., Furla, P., Houlbreque, F., Puverel, S., Reynaud, S. Tambutté, E.,
519 Tambutté, S and Zoccola, D. (2004). Biomineralisation in reef-building corals: from molecular
520 mechanisms to environmental control. *C.R. Palevol.* **3**, 453-467.
- 521 Alcazat, S.N. (1986). Observations on predators of giant clams (Bivalvia: family Tridacnidae). *Silliman*
522 *J.* **33**, 54-57.
- 523 Aldridge, D.W., Payne, B.S. and Miller, A.C. (1995). Oxygen-consumption, nitrogenous excretion, and
524 filtration-rates of *Dreissena polymorpha* at acclimation temperatures between 20 and 32
525 degrees. *Can. J. Fish. Aquat. Sci.* **52**, 1761-1767.
- 526 Armstrong, E. (2017) Ion-regulatory and developmental physiology of giant clams (Genus *Tridacna*) and
527 their conservation status on the island of Mo'orea, French Polynesia. PhD thesis, University of
528 Berkley, USA.
- 529 Andréfouët, S., Van Wynsberge, S., Gaertner-Mazouni, N., Menkes, C., Gilbert, A. and Remoissenet,
530 G. (2013). Climate variability and massive mortalities challenge giant clam conservation and
531 management efforts in French Polynesia atolls. *Biol. Conserv.* **160**,190-199.
- 532 Andréfouët, S., Dutheil, C., Menkes, C.E., Bador, M. and Lengaigne, M. (2015). Mass mortality events
533 in atoll lagoons: environmental control and increased future vulnerability. *Glob. Chang. Biol.* **21**,
534 95-205.
- 535 Andréfouët, S., Van Wynsberge, S., Kabbadj, L., Wabnitz, C.C.C., Menkes, C., Tamata, T., Pahuatini,
536 M., Tetairekie, I., Teaka, I., Ah Scha, T., Teaka, T. and Remoissenet, G. (2017). Adaptative
537 management for the sustainable exploitation of lagoon resources in remote islands: lessons
538 from a massive el Nino-induced giant clam bleaching event in the Tuamotu atolls (French
539 Polynesia). *Env. Conserv.* **45**, 30-40.
- 540 Baker, A. C. (2003). Flexibility and specificity in coral-algal symbiosis: Diversity, ecology, and
541 biogeography of *Symbiodinium*. *Annu. Rev. Ecol. Evol. Syst.* **34**, 661-689.
- 542 Bell, J.D., Lane, I., Gervis, M., Soule, S. and Tafea, H. (1997) Village-based farming of the giant clam
543 *Tridacna gigas* (L.), for the aquarium market: Initial trials in Solomon Islands. *Aquacult. Res.* **28**,
544 121-128.
- 545 Blidberg, E., Elfwing, T., Planhnan, P. and Tedengren, M. (2000). Water temperature influences on
546 physiological behaviour in three species of giant clams (Tridacnidae). *Proceeding 9th*
547 *International Coral Reef Symposium*, Bali, Indonesia, 1.
- 548 Broecker, W.S., Takahashi, T., Simpson, H.J. and Peng, T.-H. (1979). Fate of fossil fuel carbon dioxide
549 and the global carbon budget. *Science* **206**, 409-418.

- 550 Bougrier, S., Geairon, P., Deslouspaoli, J.M., Bacher, C. and Jonquieres, G. (1995). Allometric
551 relationships and effects of temperature on clearance and oxygene consumption rates of
552 *Crassostrea gigas* (Thunberg). *Aquaculture* **134**, 143-154.
- 553 Buck, B.H., Rosenthal, H. and Saint-Paul, U. (2002). Effect of increased irradiance and thermal stress
554 on the symbiosis of *Symbiodinium microadriaticum* and *Tridacna gigas*. *Aquat. Living Resour.*
555 **15**, 107-117.
- 556 Caldeira, K. and Wickett, M.E. (2003). Anthropogenic carbon and ocean pH. *Nature* **425**, 365.
- 557 Chalker, B.E. and Taylor, D.L. (1975). Light-enhanced calcification, and the role of oxidative
558 phosphorylation in calcification of the coral *Acropora cervicornis*. *Proc. R. Soc. Lond.* **190**, 323-
559 331.
- 560 Chew, S.F., Koh, C.Z.Y., Hiong, K.C., Choob, C.Y.L, Wong, W.P., Neo, M.L. and Ip, Y. (2019).
561 Light-enhanced expression of Carbonic Anhydrase 4-like supports shell formation in the fluted
562 giant clam *Tridacna squamosa*. *Gene* **683**, 101-112.
- 563 Cuif, J.-P., Dauphin, Y., Freiwald, A., Gautret and P., Zibrowius, H. (1999). Biochemical markers of
564 zooxanthellae symbiosis in soluble matrices of skeleton of 24 Scleractinia species. *Comp.*
565 *Biochem. Physiol.* **123A**, 269-278.
- 566 DeBoer, T.S., Baker, A.C., Erdmann, M.V., Jones, P.R., and Barber, P.H. (2012). Patterns of
567 *Symbiodinium* distribution in three giant clam species across the biodiverse Bird's Head region
568 of Indonesia. *Mar. Ecol. Prog. Ser.* **444**, 117-132.
- 569 Downs, C.A., Fauth J.E., Halas, J.C., Dustan, P., Bemiss, J. and Woodley, C.M. (2002). Oxidative stress
570 and seasonal coral bleaching. *Free Radic. Biol. Med.* **33**, 533-543.
- 571 Dubousquet, V., Gros, E., Berteaux-Lecellier, V., Viguier, B., Raharivelomanana, P., Bertrand, C. and
572 Lecellier, G. (2016). Changes in fatty acid composition in the giant clam *Tridacna maxima* in
573 response to thermal stress. *Biol. Open.* **5**, 1400-1407.
- 574 Elfwing, T., Blidberg, E. and Tedengren, M. (2002). Physiological responses to copper in giant clams: a
575 comparison of two methods in revealing effects on photosynthesis in zooxanthellae. *Mar.*
576 *Environ. Res.* **54**, 147-155.
- 577 Fautin, D. and Buddemeier, R. (2004). Adaptive bleaching: a general phenomenon. *Hydrobiologia* **530**,
578 459-467.
- 579 Ferrier-Pages, C., Richard, C., Forcioli, D., Allemand, D., Pichon, M. and Shick, J.M. (2007). Effects of
580 temperature and UV radiation increases on the photosynthetic efficiency in four scleractinian
581 coral species. *Biol. Bulletin.* **213**, 76-87.
- 582 Fitt, W.K., Brown, B.E., Warner, M.E. and Dunne, R.P. (2001). Coral bleaching: interpretation of thermal
583 tolerance limits and thermal thresholds in tropical corals. *Coral Reefs* **20**, 51-65.
- 584 Fitzer, S. C., Phoenix, V.R., Cusack, M. and Kamenos, N. A. (2014). Ocean acidification impacts mussel
585 control on biomineralisation. *Sci. Reports* **4**, 6218.
- 586 Furla, P., Galgani, I., Durand, I. and Allemand, D. (2000). Sources and mechanisms of inorganic
587 carbon transport for coral calcification and photosynthesis. *J. Exp. Biol.* **203**, 3445-3457.

- 588 Gazeau, F., Gattuso, J., Dawber, C., Pronker, A., Peene, F., Peene, J., Heip, C. and Middelburg, J.
589 (2010) Effect of ocean acidification on the early life stages of the blue mussel *Mytilus edulis*.
590 *Biogeosciences* **7**, 2051-2060.
- 591 Gazeau, F., Parker, L.M., Comeau, S., Gattuso, J., O'Connor, W., Martin, S., Portner, H. and Ross, P.M.
592 (2013). Impacts of ocean acidification on marine shelled molluscs. *Mar. Biol.* **160**, 2207-2245.
- 593 Goreau, T.F. (1959). The physiology of skeleton formation in corals. I. A method for measuring the rate
594 of calcium deposition by corals under different conditions. *Biol. Bull.* **116**, 59-75.
- 595 Hawkins, A.J.S. and Klumpp, D.W. (1995) Nutrition of the giant clam *Tridacna gigas* (L.). II. Relative
596 contributions of filter-feeding and the ammonium-nitrogen acquired and recycled by symbiotic
597 alga towards total nitrogen requirements for tissue growth and metabolism. *J. Exp. Mar. Biol.*
598 *Ecol.* **190**, 263-290.
- 599 Harper, E.M. (2000). Are calcitic layers an effective adaptation against shell dissolution in the Bivalvia?
600 *J. Zool.* **251**, 179e186.
- 601 Hoegh-Guldberg, O., Mumby, P.J., Hooten, A.J., Steneck, R.S., Greenfield, P., Gomez, E., Harvell,
602 C.D., Sale, P.F., Edwards, A.J., Caldeira, et al. (2007). Coral reefs under rapid climate change
603 and ocean acidification. *Science* **318**, 1737-1742.
- 604 Holcomb, M., Venn, A., Tambutté, E., Tambutté, S., Allemand, D., Trotter, J. and McCulloch, M. (2014).
605 Coral calcifying fluid pH dictates response to ocean acidification. *Sci. Reports* **4**, 5207.
- 606 Holt, A.L., Vahidinia, S., Gagnon, Y.L., Morse, D.E. and Sweeney, A.M. (2014). Photosymbiotic giant
607 clams are transformers of solar flux. *J. Royal Soc. Interface* **11**, 20140678.
- 608 Ikeda, S., Yamashita, H., Kondo, S., Inoue, K., Morishima, S., Koike, K. (2017). Zooxanthellal genetic
609 varieties in giant clams are partially determined by species-intrinsic and growth-related
610 characteristics. *PLoS One* **12**, e0172285.
- 611 Ip, Y.K., Loong, A.M., Hiong, K.C., Wong, W.P., Chew, S.F., Reddy, K., Sivaloganathan, B. and
612 Ballantyne, J.S. (2006). Light induces an increase in the pH of and a decrease in the ammonia
613 concentration in the extrapallial fluid of the giant clam *Tridacna squamosa*. *Physiol. Biochem.*
614 *Zool.* **79**, 656-664.
- 615 Ip, Y.K., Hiong, K.C., Goh, E.J.K., Boo, M.V., Choo, Y.L., Ching, B., Wong, W.P. and Chew, S.F. (2017).
616 The whitish inner mantle of the giant clam, *Tridacna squamosa*, expresses an apical Plasma
617 Membrane Ca²⁺-ATPase (PMCA) which displays light-dependent gene and protein
618 expressions. *Front. Physiol.* **8**, 781.
- 619 IPCC (2014). Summary for policymakers. In *Climate Change 2014: Impacts, Adaptation, and*
620 *Vulnerability. Part A: Global and Sectoral Aspects. Contribution of Working Group II to the Fifth*
621 *Assessment Report of the Intergovernmental Panel on Climate Change* (ed. C.B. Field, V.R.
622 Barros, D.J. Dokken, K.J. Mach, M.D. Mastrandrea, T.E. Bilir, M. Chatterjee, K.L. Ebi, Y.O.
623 Estrada, R.C. Genova, B. Girma, E.S. Kissel, A.N. Levy, S. MacCracken, P.R. Mastrandrea and
624 L.L. White), pp. 1-32. Cambridge, UK and New York, NY, USA: Cambridge University Press.

- 625 IPCC (2018) Summary for Policymakers. In *Global warming of 1.5°C. An IPCC Special Report on the*
626 *impacts of global warming of 1.5°C above pre-industrial levels and related global greenhouse*
627 *gas emission pathways, in the context of strengthening the global response to the threat of*
628 *climate change, sustainable development, and efforts to eradicate poverty.* (ed. V. Masson-
629 Delmotte, P. Zhai, H. O. Pörtner, D. Roberts, J. Skea, P. R. Shukla, A. Pirani, W. Moufouma-
630 Okia, C. Péan, R. Pidcock, S. Connors, J. B. R. Matthews, Y. Chen, X. Zhou, M. I. Gomis, E.
631 Lonnoy, T. Maycock, M. Tignor, T. Waterfield), pp. 1-32. World Meteorological Organization,
632 Geneva, Switzerland.
- 633 Ishikura, M., Adachi, K. and Maruyama, T. (1999). Zooxanthellae release glucose in the tissue of a giant
634 clam, *Tridacna crocea*. *Mar. Biol.* **133**, 665-673.
- 635 Jones, R.J. and Hoegh-Guldberg, O. (2001). Diurnal changes in the photochemical efficiency of the
636 symbiotic dinoflagellates (*Dinophyceae*) of corals: photoprotection, photoinactivation and the
637 relationship to coral bleaching. *Plant Cell and Environ.* **24**, 89-99.
- 638 Junchompoo, C., Sinrapasan, N., Penpain, C. and Patsorn, P. (2013). Changing seawater temperature
639 effects on giant clams bleaching, Mannai Island, Rayong province, Thailand. *Proceedings of the*
640 *Design Symposium on Conservation of Ecosystem* (The 12th SEASTAR2000 workshop), 71-
641 76.
- 642 Kleypas, J. A. (1999). Geochemical Consequences of Increased Atmospheric Carbon Dioxide on Coral
643 Reefs. *Science* **284**, 118-120.
- 644 Klumpp, D.W., Bayne, B.L. and Hawkins, A.J.S. (1992). Nutrition of the giant clam *Tridacna gigas*.
645 Contribution of filter feeding and photosynthates to respiration and growth. *J. Exp. Mar. Biol.*
646 *Ecol.* **155**, 105-122.
- 647 Klumpp, D.W. and Griffiths, C.L. (1994). Contributions of phototrophic and heterotrophic nutrition to the
648 metabolic and growth requirements of four species of giant clam (*Tridacnidae*). *Mar. Ecol. Prog.*
649 *Ser.* **115**, 103-115.
- 650 Klumpp, D.W. and Lucas, J.S. (1994). Nutritional ecology of the giant clams *Tridacna tevoroa* and *T.*
651 *derasa* from Tonga – Influence of light on filter-feeding and photosynthesis. *Mar. Ecol. Prog.*
652 *Ser.* **107**, 147-156.
- 653 Kroeker, K.J., Kordas, R.L., Crim, R.N. and Singh, G.G. (2010). Meta-analysis reveals negative yet
654 variable effects of ocean acidification on marine organisms. *Ecol. Letters.* **13**, 1419-1434.
- 655 Kurihara, H. (2008). Effects of CO₂-driven ocean acidification on the early developmental stages of
656 invertebrates. *Mar. Ecol. Prog. Ser.* **373**, 275-284.
- 657 Kurihara, T., Yamada, H., Inoue, K., Iwai, K. and Hatta, M. (2013). Impediment to symbiosis
658 establishment between giant clams and *Symbiodinium* algae due to sterilization of seawater.
659 *PLoS One* **8**, e61156.
- 660 LaJeunesse, T. C., Parkinson, J. E., Gabrielson, P. W., Jeong, H. J., Reimer, J. D., Voolstra, C. R., and
661 Santos, S. R. (2018). Systematic revision of Symbiodiniaceae highlights the antiquity and
662 diversity of coral endosymbionts. *Current Biology* **28**, 2570-2580.e6.

- 663 Latchère, O., le Moullac, G., Gaetner-Mazouni, N., Fievet, J., Magré, K. and Saulnier, D. (2017).
664 Influence of preoperative food and temperature conditions on pearl biogenesis in *Pinctada*
665 *margaritifera*. *Aquaculture* **479**, 176-187.
- 666 Leggat, W., Buck, B.H., Grice, A. and Yellowlees, D. (2003). The impact of bleaching on the metabolic
667 contribution of dinoflagellate symbionts to their giant clam host. *Plant Cell Environ.* **26**, 1951-
668 1961.
- 669 Le Moullac, G., Soyez, C., Latchere, O., Vidal-Dupiol, J., Fremery, J., Saulnier, D., Lo Yat, A., Belliard,
670 C., Mazouni-Gaertner N., and Gueguen, Y. (2016a). *Pinctada margaritifera* responses to
671 temperature and pH: acclimation capabilities and physiological limits. *Estuar. Coast Shelf Sci.*
672 **182**, 261-269.
- 673 Le Moullac, G., Soyez C., Vidal-Dupiol, J., Belliard, C., Fievet, J. Sham-Koua, M., Lo Yat, A., Saulnier,
674 D., Gaertner-Mazouni, N. et al. (2016b). Impact of pCO₂ on the energy, reproduction and growth
675 of the shell of the pearl oyster *Pinctada margaritifera*. *Estuar. Coast Shelf Sci.* **182**, 274-282.
- 676 Lesser, M.P. (1996). Elevated temperatures and ultraviolet radiation cause oxidative stress and inhibit
677 photosynthesis in symbiotic dinoflagellates. *Limnol. Oceanog.* **41**, 271-283.
- 678 Lesser, M.P., Stochaj, W.R., Tapley, D.W. and Schick, J.M. (1990). Bleaching in coral reef anthozoans:
679 Effects of irradiance, ultraviolet radiation and temperature on the activities of protective enzymes
680 against active oxygen. *Coral Reefs* **8**, 225-232.
- 681 Lim, S.S.Q., Huang, D., Soong, K., and Neo, M.L. (2019). Diversity of endosymbiotic Symbiodiniaceae
682 in giant clams at Dongsha Atoll, northern South China Sea. *Symbiosis* doi:10.1007/s13199-019-
683 00615-5.
- 684 Lin, A.Y.M., Meyers, M.A. and Vecchio, K.S. (2006). Mechanical properties and structure of *Strombus*
685 *gigas*, *Tridacna gigas*, and *Haliotis rufescens* sea shells: a comparative study. *Mater. Sci. Eng.*
686 *A. Struct. Mater.* **26**, 1380-1389.
- 687 Liu, W., Huang, X., Lin, J. and He, M. (2012). Seawater acidification and elevated temperature affect
688 gene expression patterns of the pearl oyster *Pinctada fucata*. *PLoS One* **7**, e33679.
- 689 Lucas, J.S. (1994). The biology, exploitation, and mariculture of giant clams (*Tridacnidae*). *Rev.*
690 *Fisheries Science* **2**, 181-223.
- 691 Marin, F., Le Roy, N. and Marie, B. (2012). Formation and mineralization of mollusk shell. *Front. Biosci.*
692 **4**, 1099-1125.
- 693 McCulloch, M., Falter, J., Trotter, J. and Montagna, P. (2012). Coral resilience to ocean acidification and
694 global warming through pH up-regulation. *Nature Clim. Change* **2**, 623-627.
- 695 Melzner, F., Stange, P., Trübenbach, K., Thomsen, J., Casties, I., Panknin, U., Gorb, S. and Gutowska,
696 M. (2011) Food Supply and Seawater pCO₂ Impact Calcification and Internal Shell Dissolution
697 in the Blue Mussel *Mytilus edulis*. *PLoS One* **6**, e24223.
- 698 Mies, M., Dor, P., Güth, A.Z. and Sumida, P.Y.G. (2017). Production in giant clam aquaculture: Trends
699 and Challenges. *Rev. Fish. Sci. Aquac.* **25**, 286-296.

- 700 Milano, S., Schöne, B.R., Wang, S. and Müller, W.E. (2016). Impact of high pCO₂ on shell structure of
701 the bivalve *Cerastoderma edule*. *Mar. Envir. Res.* **119**, 144-155.
- 702 Muscatine, L., Goiran, C., Land, L., Jaubert, J., Cuif, J.P. and Allemand, D. (2005). Stable isotopes
703 (δ C-13 and δ N-15) of organic matrix from coral skeleton. *Proc. Nation. Acad. Sci. USA.*
704 **102**, 1525-1530.
- 705 Neo, M.L., Eckman, W., Vicentuan, K., Teo, S.L.M. and Todd, P.A. (2015). The ecological significance
706 of giant clams in coral reef ecosystems. *Biol. Conserv.* **181**,111-123.
- 707 Norton, J.H., Shepherd, M.A., Long, H.M. and Fitt, W.K. (1992). The zooxanthellal tubular system in the
708 giant clam. *Biol Bull.* **183**, 503-506.
- 709 Orr, J.C., Fabry, V.J., Aumont, O., Bopp, L., Doney, S.C., Feely, R.A., Gnanadesikan, A., Gruber, N.,
710 Ishida, A., Joos, F. et al. (2005). Anthropogenic ocean acidification over the twenty-first century
711 and its impact on calcifying organisms. *Nature* **437**, 681-686.
- 712 Palmer, A.R. (1992). Calcification in marine molluscs: how costly is it? *Proc. Natl. Acad. Sci. USA.* **89**,
713 1379-1382.
- 714 Pätzold, J., Heinrichs, J.P., Wolschendorf, K. and Wefer, G. (1991). Correlation of stable oxygen isotope
715 temperature record with light attenuation profiles in reef-dwelling *Tridacna* shells. *Coral Reefs*
716 **10**, 65- 69.
- 717 Pearse, V.B. and Muscatine, L. (1971). Role of symbiotic algae (zooxanthellae) in coral calcification.
718 *Biol. Bull.* **141**, 350-363.
- 719 Perez, S. and Weis, V. (2006). Nitric oxide and cnidarian bleaching: an eviction notice mediates
720 breakdown of a symbiosis. *J. Exp. Biol.* **209**, 2804-2810.
- 721 Pinzón, J.H., Devlin-Durante, M.K., Weber, M.X., Baums, I.B., and LaJeunesse, T.C. (2011).
722 Microsatellite loci for *Symbiodinium* A3 (*S. fitti*) a common algal symbiont among Caribbean
723 *Acropora* (stony corals) and Indo-Pacific giant clams (*Tridacna*). *Conserv. Genet. Resour.* **3**,
724 45-47.
- 725 Richier, S., Sabourault, C., Courtiade, J., Zucchini, N., Allemand, D. and Furla, P. (2006). Oxidative
726 stress and apoptotic events during thermal stress in the symbiotic sea anemone, *Anemonia*
727 *viridis*. *Febs Journal* **273**, 4186-4198.
- 728 Richter C, Rühle, W. and Wild, A. (1990). Studies on the mechanisms of photosystem II photoinhibition
729 II. The involvement of toxic oxygen species. *Photosynthesis Res.* **24**, 237-243.
- 730 Ries, J.B., Cohen, A.L. and McCorkle, D.C. (2009). Marine calcifiers exhibit mixed responses to CO₂-
731 induced ocean acidification. *Geology* **37**, 1131-1134.
- 732 Ries, J.B. (2011) A physiochemical framework for interpreting the biological calcification response to
733 CO₂-induced ocean acidification. *Geochim Cosmochim Acta* **75**, 4053-4064.
- 734 Rodolfo-Metalpa, R., Houlbreque, F., Tambutte, E., Boisson, F., Baggini, C., Patti, F.P., Jeffree, R.,
735 Fine, M., Foggo, A., Gattuso, J.P. et al. (2011). Coral and mollusc resistance to ocean
736 acidification adversely affected by warming. *Nature Clim. Change* **1**, 308-312.

- 737 Sabine, C.L., Feely, R.A., Gruber, N., Key, R.M., Lee, K., Bullister, J.L., Wanninkhof, R., Wong, C.S.,
738 Wallace, D.W.R., Tilbrook, B. et al. (2004). The oceanic sink for anthropogenic CO₂. *Science*
739 **305**, 367-371.
- 740 Schwartzmann, C., Durrieu, M., Sow, M., Ciret, P., Lazareth, C.E. and Massabuau, J.-C. (2011) In situ
741 giant clam growth rate behavior in relation to temperature: A one-year couple study of high-
742 frequency noninvasive valvometry and sclerochronology. *Limnol. Ocean.* **56**, 1940-1951.
- 743 Smith, D.J., Suggett, D.J. and Baker, N.R. (2005). Is photoinhibition of zooxanthellae photosynthesis
744 the primary cause of thermal bleaching in corals? *Global Change Biology* **11**, 1-11.
- 745 Soo, P. and Todd, P.A. (2014). The behaviour of giant clams. *Mar. Biol.* **161**, 2699-2717.
- 746 Talmage, S.C. and Gobler, C.J. (2011). Effects of elevated temperature and carbon dioxide on the
747 growth and survival of larvae and juveniles of three species of northwest Atlantic bivalves. *PLoS*
748 *One* **6**, e26941.
- 749 Toonen, R.J., Nakayama, T., Ogawa, T., Rossiter, A. and Delbeek, J.C. (2012). Growth of cultured giant
750 clams (*Tridacna spp.*) in low pH, high nutrient seawater: species-specific effects of substrate
751 and supplemental feeding under acidification. *J. Mar. Biol. Assoc. UK.* **92**, 731-740.
- 752 Vandermeulen, J.H., Davis, N.D. and Muscatine, L. (1972). The effect of inhibitors of photosynthesis on
753 zooxanthellae in corals and other marine invertebrates. *Mar. Bio.* **16**, 185-191.
- 754 van Heuven, S., Pierrot, D., Lewis, E. and Wallace, D.W.R. (2009). MATLAB Program developed for
755 CO₂ system calculations, ORNL/CDIAC-105b, Carbon Dioxide Information Analysis Center,
756 Oak Ridge National Laboratory, US Department of Energy, Oak Ridge, Tennessee.
- 757 Van Wynsberge, S., Andréfouët, S., Gaertner-Mazouni, N., Wabnitz, C.C.C., Gilbert, A., Remoissenet,
758 G., Payri, C. and Fauvelot, C. (2016). Drivers of density for the exploited giant clam *Tridacna*
759 *maxima*: a meta-analysis. *Fish Fish.* **17**, 567-584.
- 760 Venn, A., Tambutté, E., Holcomb, M., Laurent, J., Allemand, D. and Tambutté, S. (2013). Impact of
761 seawater acidification on pH at the tissue-skeleton interface and calcification in reef corals.
762 *PNAS* **110**, 1634-1639.
- 763 Warner, M.E., Fitt, W.K., and Schmidt, G.W. (1999). Damage to photosystem II in symbiotic
764 dinoflagellates: A determinant of coral bleaching. *Proc. Natl. Acad. Sci.* **96**, 8007-8012.
- 765 Waters, C.G. (2008). Biological responses of juvenile *Tridacna maxima* (Mollusca:Bivalvia) to increased
766 pCO₂ and ocean acidification. Master thesis, The Evergreen State College.
- 767 Watson, S.-A., Southgate, P.C., Miller, G.M., Moorhead, J.A. and Knauer, J. (2012). Ocean acidification
768 and warming reduce juvenile survival of the fluted giant clam *Tridacna squamosa*. *Molluscan*
769 *Res.* **32**, 177-180.
- 770 Watson, S. (2015). Giant Clams and rising CO₂: Light may ameliorate effects of ocean acidification on
771 a solar-powered animal. *PLoS One* **10**, e0128405.
- 772 Welladsen, H.M., Southgate, P.C. and Heimann, K. (2010). The effects of exposure to near-future levels
773 of ocean acidification on shell characteristics of *Pinctada fucata* (Bivalvia: Pteriidae). *Molluscan*
774 *Res.* **30**, 125-130.

- 775 Yau, A.J.Y. and Fan, T.Y. (2012). Size-dependent photosynthetic performance in the giant clam
776 *Tridacna maxima*, a mixotrophic marine bivalve. *Mar. Biol.* **159**, 65-75.
- 777 Zeebe, R.E., Zachos, J.C., Caldeira, K. and Tyrrell, T. (2008). Oceans-Carbon emissions and
778 acidification. *Science* **321**, 51-52.
- 779 Zhou, Z., Liu, Z., Wang, L., Luo, J. and Li, H. (2019) Oxidative stress, apoptosis activation and symbiosis
780 disruption in giant clam *Tridacna crocea* under high temperature. *Fish. Fish. Immunol.* **84**, 451-
781 457.

782 **Figure and table legends**

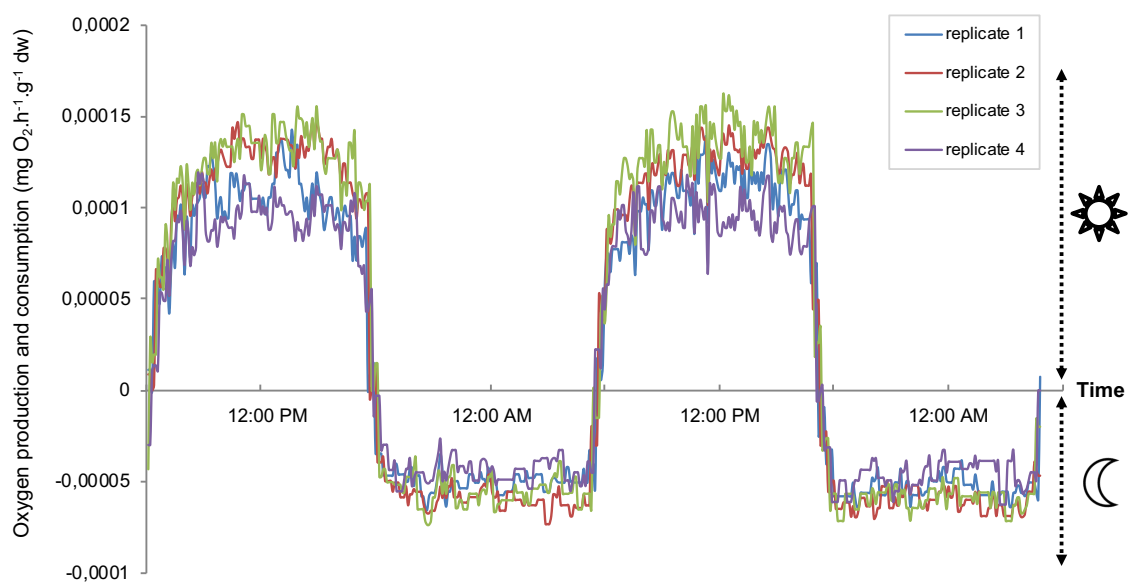
783

784 **Table 1. Measured and calculated parameters of seawater for all treatments.** Total alkalinity is
785 given in mean (\pm s.d.) based on weekly measurements for each experimental tank corresponding to
786 $n=36$ for each condition. $p\text{CO}_2$ and $\Omega_{\text{aragonite}}$ were calculated using the CO₂ Systat software.

787

Treatments	Temperature (°C)	$p\text{CO}_2$ (μatm)	pH_{NBS}	Salinity (‰)	Total alkalinity ($\mu\text{mol/kg SW}$)	$\Omega_{\text{aragonite}}$
Control	29.2 (\pm 0.1)	428 (\pm 21)	8.19 (\pm 0.01)	35	2422 (\pm 170)	4.17
Thermal stress	30.7 (\pm 0.1)	431(\pm 25)	8.19 (\pm 0.01)	35	2409 (\pm 157)	4.14
Acidification stress	29.2 (\pm 0.1)	1210 (\pm 41)	7.81 (\pm 0.03)	35	2466 (\pm 90)	1.99
Acidification and thermal stress	30.7 (\pm 0.1)	1213 (\pm 29)	7.81 (\pm 0.03)	35	2423 (\pm 110)	2.02

788



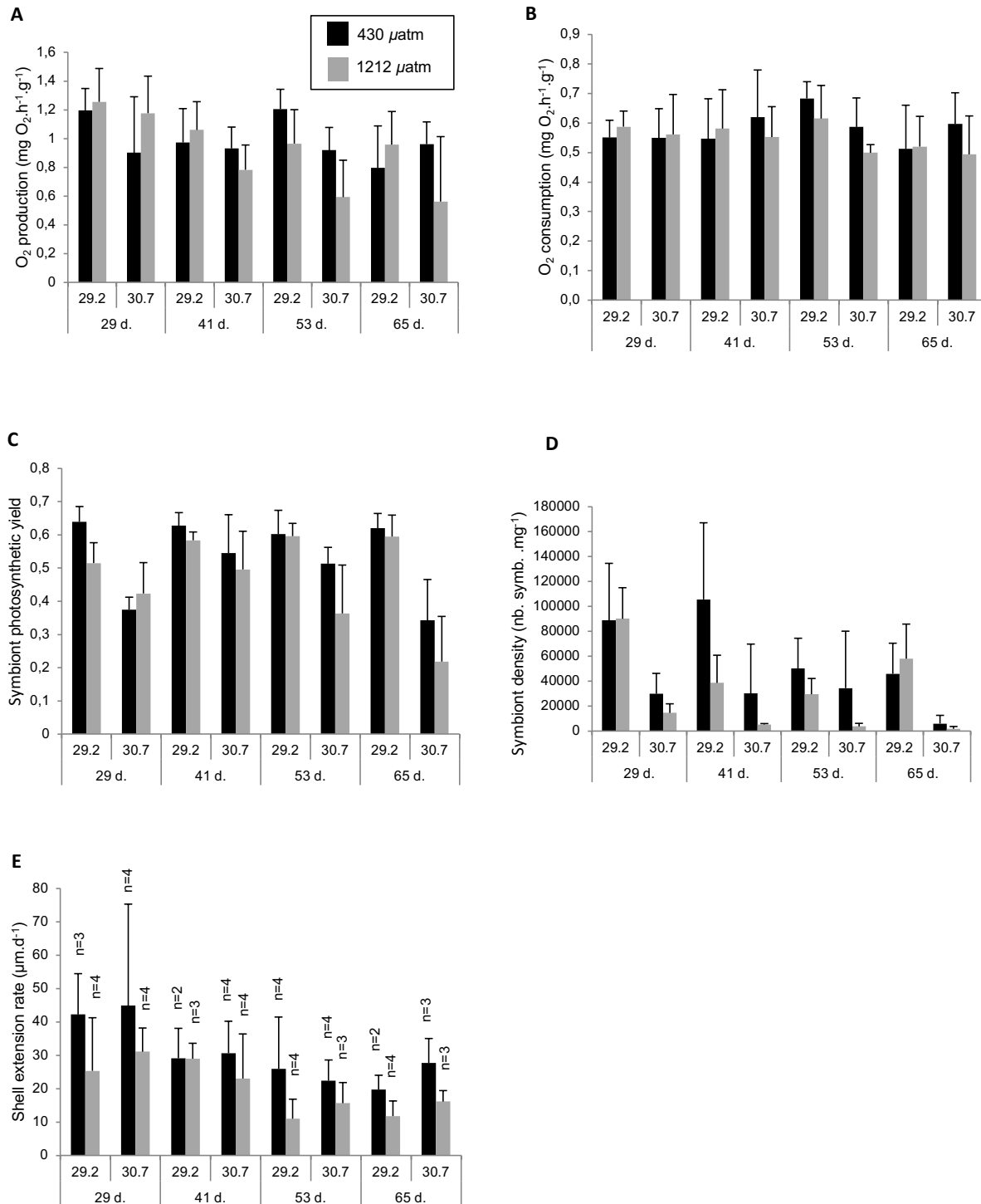
789

790 **Figure 1. Variations of oxygen consumption and oxygen production acquired over a 48 h period**

791 **after 29 days of exposure to 29.2°C and 430 μ atm of CO₂.** Data are expressed in mg O₂.h⁻¹.g⁻¹ tissue

792 dry weight (dw) and correspond to day-time and night-time acquisitions for 4 giant clam replicates.

793



794

795 **Figure 2. Graphs reporting data of (A) oxygen production, (B) oxygen consumption, (C) symbiont**
 796 **photosynthetic yield and (D) density, and (E) daily shell extension rate obtained for each**
 797 **temperature/ $p\text{CO}_2$ experimental condition and time of exposure. Black and grey columns**
 798 **correspond to today $p\text{CO}_2$ condition (430 μatm) and future $p\text{CO}_2$ condition (1212 μatm), respectively.**
 799 **Data are given in mean (+s.d.) calculated from 4 replicates (n=4) for each physiological parameter**
 800 **excepted for daily shell extension rate. For this latter parameter, numbers of replicates are indicated on**
 801 **the graph.**

802

803 **Table 2. Results from the three-way ANOVA performed on holobiont O₂ production and**
 804 **consumption data, symbiont photosynthetic yield, symbiont density, and giant clam shell**
 805 **extension rate.** The three fixed factors are pCO₂, temperature and time of exposure.
 806 Significant differences ($P < 0.05$) are highlighted in grey.
 807

		O ₂ production (n=64)	O ₂ consumption (n=64)	Photosynthetic yield (n=64)	Symbiont density (n=64)	Shell extension rate (n=55)
Time	<i>F</i>	3.264	0.740	3.566	6.035	4.695
	<i>P</i>	0.030	0.533	0.021	0.001	0.007
Temperature	<i>F</i>	7.551	0.294	65.200	79.158	0.466
	<i>P</i>	0.009	0.590	<0.0001	<0.0001	0.499
pCO₂	<i>F</i>	0.846	0.851	6.125	8.665	7.409
	<i>P</i>	0.362	0.361	0.017	0.005	0.010
Time x Temperature	<i>F</i>	0.413	0.965	3.393	1.528	0.319
	<i>P</i>	0.744	0.417	0.025	0.219	0.812
Time x pCO₂	<i>F</i>	1.765	0.476	0.024	1.033	0.251
	<i>P</i>	0.167	0.700	0.995	0.386	0.860
Temperature x pCO₂	<i>F</i>	1.334	1.029	0.100	1.989	0.026
	<i>P</i>	0.254	0.315	0.753	0.165	0.872
Time x Temperature x pCO₂	<i>F</i>	1.216	0.148	2.153	0.474	0.336
	<i>P</i>	0.314	0.930	0.106	0.702	0.799

808

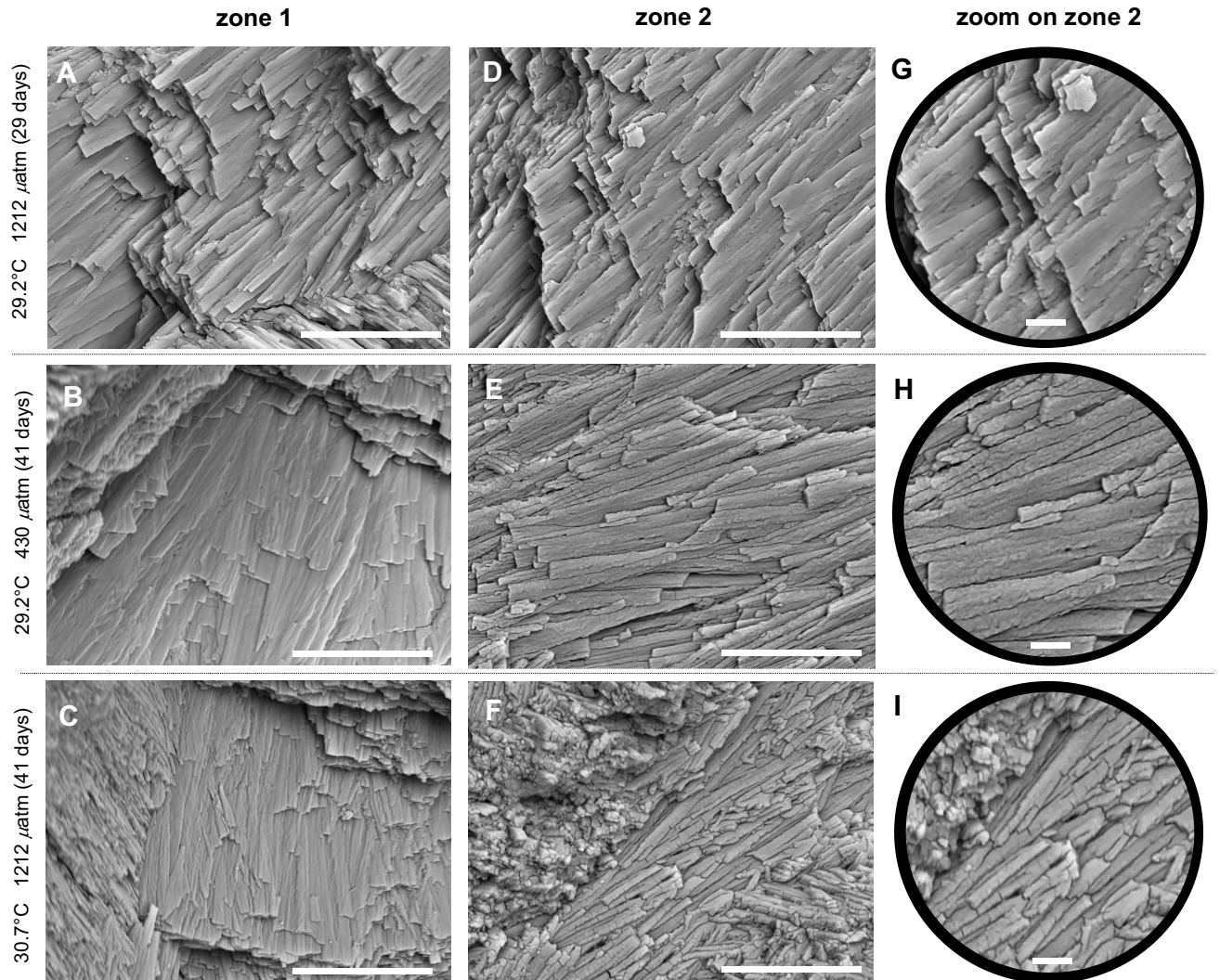
809 **Table 3. Results from Tukey post hoc tests following the three-way ANOVA performed on**
 810 **analyzed physiological parameters.** The effects of significant parameters were tested as time of
 811 exposure alone and combined to the temperature. The letter annotations correspond to the significances
 812 between conditions ($P < 0.005$).
 813

		O ₂ production	Photosynthetic yield	Symbiont density	Shell extension rate
Time	29 d.	a	a	a	a
	41 d.	ab	ab	ab	ab
	53 d.	ab	ab	b	b
	65 d.	b	b	b	b
Temperature	29.2°C	a	a	a	-
	30.7°C	b	b	b	-
pCO₂	430 μ atm	-	a	a	a
	1212 μ atm	-	b	b	b
Time x Temperature	29 d. x 29.2°C	-	ab	-	-
	41 d. x 29.2°C	-	a	-	-
	53 d. x 29.2°C	-	a	-	-
	65 d. x 29.2°C	-	a	-	-
	29 d. x 30.7°C	-	cd	-	-
	41 d. x 30.7°C	-	abc	-	-
	53 d. x 30.7°C	-	bcd	-	-
	65 d. x 30.7°C	-	d	-	-

814

815 **Table 4. Correlation matrix integrating the different physiological parameters monitored, i.e., O₂**
816 **production and consumption, shell extension rate and symbiont photosynthetic yield and**
817 **density.** Correlation were tested using the Pearson method (threshold of $r=0.250$, $\alpha=0.05$) and
818 significant relationships between parameters are highlighted in grey.

	Photosynthetic yield (n=64)	Symbiont density (n=64)	Shell extension rate (n=55)	O₂ production (n=64)
Symbiont density	0.667			
Shell extension rate	-0.032	0.168		
O ₂ production	0.331	0.492	0.221	
O ₂ consumption	0.163	0.226	0.129	0.629



819

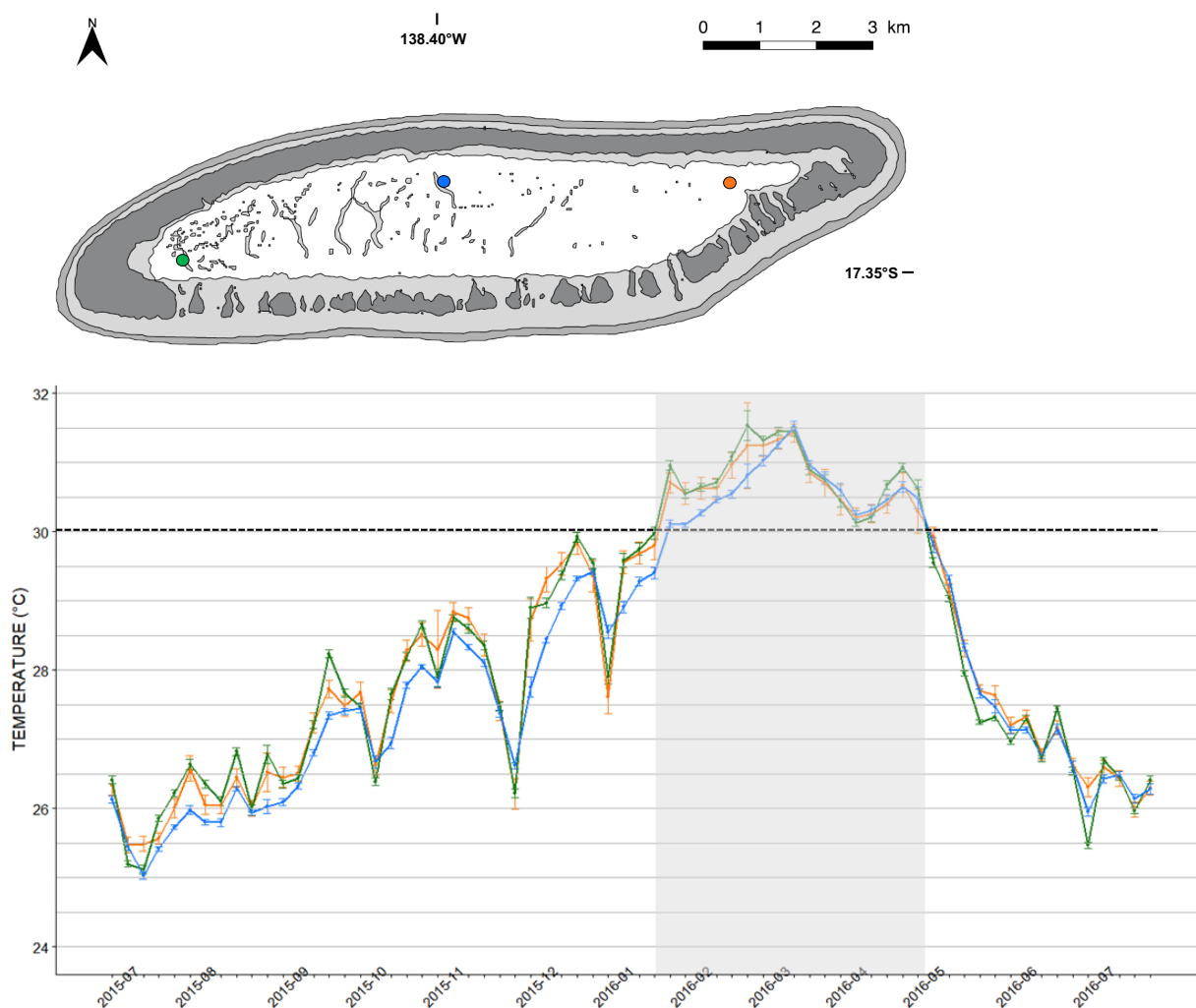
820 **Figure 3. Effects of experimental conditions on the ultrastructure of the *Tridacna maxima* shell**
821 **outer layer investigated via scanning electron microscopy.** (A-F: scale bar: 10 μ m, G-I: scale bar:
822 2 μ m). Zone 1 and zone 2 correspond to the shell formed *in situ* (i.e., before the experiment) and in the
823 experimental conditions, respectively. (A, B and G): 29.2°C 1212 μ atm (29 days): no difference between
824 zone 1 and 2. In both zones, lamellae are well-cohesive, displaying elongated shape with a smooth
825 surface and slightly rounded outlines. (B, E and H) 29.2°C 430 μ atm (41 days): lamellae in zone 2 are
826 less-cohesive, with a pronounced granular aspect. (C, F and I) 30.7°C 430 μ atm (41 days): lamellae in
827 zone 2 are less-cohesive and display crazes.

828

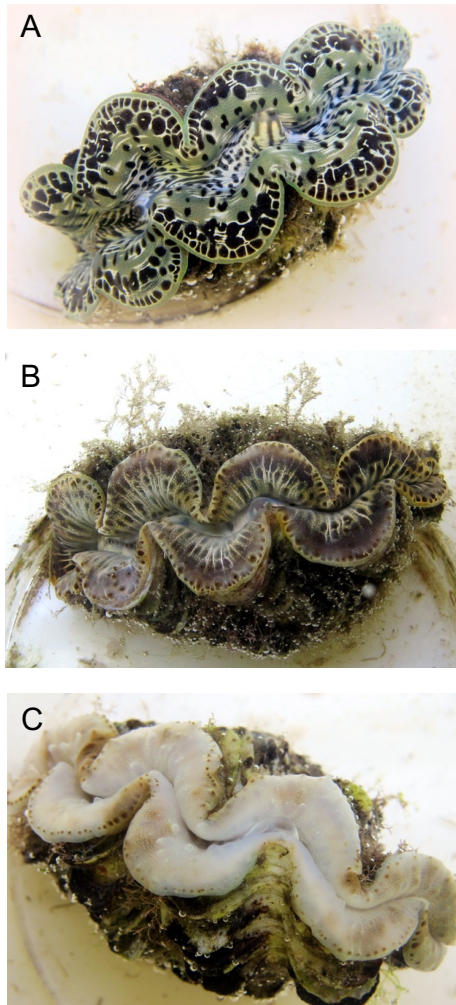
829 **Table 5. Compilation of ultrastructural observations of the lamellae of the shell outer layer using**
 830 **scanning electron microscopy.** “ND” means that no significant difference is observed between the
 831 shell formed before and during the experiment. “D” means that a notable difference is observed between
 832 both parts of the shell. “A” and “B” represent the two samples observed for each treatment and time of
 833 exposure.
 834

Time of exposure	Temperature (°C)	pCO ₂ (μatm)	Sample	Difference
29 d.	29.2	430	A	ND
			B	ND
	30.7	430	A	ND
			B	ND
	29.2	1212	A	ND
			B	ND
	30.7	1212	A	ND
			B	ND
41 d.	29.2	430	A	D
			B	D
	30.7	430	A	D
			B	D
	29.2	1212	A	D
			B	D
	30.7	1212	A	D
			B	ND
53 d.	29.2	430	A	D
			B	D
	30.7	430	A	D
			B	D
	29.2	1212	A	ND
			B	D
	30.7	1212	A	D
			B	ND
65 d.	29.2	430	A	D
			B	D
	30.7	430	A	D
			B	ND
	29.2	1212	A	D
			B	D
	30.7	1212	A	ND
			B	D

835 **Supplementary Material**
836



837
838 **Figure S1. *In situ* seawater temperatures recorded from July 2015 to July 2016 inside the lagoon**
839 **of Tatakoto atoll (Tuamotu islands) at 2 m depth.** Temperature were recorded using UA-002-64
840 HOBO Onset data loggers. Curves on the graph report data from 3 sites localized on the map by circles
841 with corresponding color. Grey rectangle highlights the period when giant clams were exposed to a
842 temperature $\geq 30^{\circ}\text{C}$.



843

844 **Figure S2. Visual observation of bleaching in giant clam *Tridacna maxima* specimens after 65**

845 **days in experimental conditions. (A) Non-bleached specimen exposed to 29.2°C 430 μ atm of CO₂,**

846 **(B) partially bleached and (C) completely bleached specimens exposed to 30.7°C 1212 μ atm of CO₂.**